Stark shifts, band-edge transitions, and intrinsic optical dipoles in spherical InP quantum dots under electric fields

Huaxiang Fu
Department of Physics, Rutgers University, Camden, New Jersey 08102
(Received 6 August 2001; published 7 January 2002)

The band-edge electronic structure of spherical InP dots under electric fields is investigated using an atomistic pseudopotential approach. Field-induced changes in orbital energies, single-particle wave functions, transition intensities, and excitonic gaps are calculated. We find that interstate couplings profoundly affect the Stark shifts and optical transitions in InP quantum dots. As a result, band-edge transitions can be enhanced instead of being quenched by the field. We also demonstrate that both dipole and polarizability contributions should exist in the Stark shifts of zinc-blende dots.

DOI: 10.1103/PhysRevB.65.045320 PACS number(s): 73.22.−f, 78.67.−n

Semiconductor colloidal dots are special because of their variety of size-tunable physical properties such as excitonic gap,[1] electron-hole exchange interaction,[2] and solid-to-solid phase transition pressure.[3] Recently, much attention[4–7] has been paid to semiconductor dots under electric fields, in which the ultranarrow single-dot luminescence linewidth[6] and the fast carrier response could lead to better performances in devices such as optical switches. Electric fields applied to quantum-confined semiconductor systems will cause drastic changes in band-edge transitions by polarizing the electron and hole wave functions.[8] As a result, the photoluminescence peak position will be shifted (i.e., the Stark shift) and the intensity will be weakened. In CdSe dots of an average diameter $D=75$ Å, Stark shifts as large as 50 meV were observed[6] under a field of ~ 300 kV/cm. Importantly, a *single-dot* Stark shift of CdSe was found to have both dipolar and polarizable components.[6] Under the assumption that there are dipole as well as polarizability contributions, the Stark shift of the excitonic transition energy ($\Delta\omega_{\rm gap}^{\rm ex}$) can be generally formulated (in the SI unit system) as a function of the field strength (E) using

$$\Delta\omega_{\rm gap}^{\rm ex}=\mu E+\frac{1}{2}\alpha\epsilon_0 E^2, \tag{1}$$

where μ and α are the dipole and polarizability of a single dot, respectively. ϵ_0 is the permittivity of the free space. Here we use ω to denote the energy gap, to be differentiated from the single-particle orbital energy notation ε (see below). It has been realized[5,6] that in *ensembled* CdSe dots only the polarizability contribution [i.e., the second term in Eq. (1)] is likely to be observed, since the random dipole orientations in different dots may result in a zero net dipole. While the dipolar character of Stark shifts in CdSe dots is understandable as a result of the wurzite structure of CdSe, it has been speculated that there will be a nominal dipole character in zinc-blende dots. So far there is no single-dot experimental data on the Stark effect in zinc-blende dots.

It should also be pointed out that the implications of the Stark effect in quantum dots are not limited to cases when external electric fields are applied to the dots. Recent experiments[9] demonstrated that photoionizations[10,11] will generate additional positive charges in dots. These positive charges will cause an internal electric field, which could be much larger than the typical external field (~ 300 kV/cm). As simulated by Wang[12] for CdSe dots, a point charge near the boundary of dot will dramatically quench the band-edge transitions. In consideration of the great deal of experimental interest in colloidal dots under electric fields, it is desirable to have a theoretical understanding of the electric-field effect on the electronic structure of semiconductor colloidal dots.

Here we theoretically study the band-edge states of InP quantum dots under electric fields, using an atomistic pseudopotential approach.[13] The high-quality wave functions offered by our approach allow us to calculate accurately the electron-hole Coulomb energies which will be shown to be significant in determining the Stark shifts in dots. Our calculations are performed for InP dots with sizes in the experimental range (i.e., from 20 to 60 Å in diameter). For these dots in the strong-confinement regime, the energy spacings between different states ($\geqslant 50$ meV) are much larger than the typical Stark shifts (~ 10 meV). We will thus focus our attention on a few important states near the band edge, e.g., the conduction-band minimum (CBM), the valence-band maximum (VBM), and the next valence state below the VBM (hereafter named the VBM-1 state). We find that the VBM of an InP dot is much more strongly polarized than the CBM. Unlike the VBM, that is oppositely polarized in comparison with the CBM, the VBM-1 in a spherical InP dot is, rather unexpectedly, polarized along the same direction as the CBM. As a consequence, if a polarized excitation along the field direction is conducted, the transition intensity between the VBM-1 and CBM states will be enhanced (instead of being weakened) by the electric field. Our calculations show that the Stark shift of the *excitonic* gap in a quantum dot is much smaller than the field-induced reduction of the single-particle band gap, and the latter should not be directly compared to the shift of luminescence peak observed in experiments. Interestingly, our calculations demonstrate that the optical dipole μ in Eq. (1) is nonzero even for the spherical InP dots; this conclusion should be valid for all zinc-blende dots.

The single-particle orbital energies $\{\varepsilon_i\}$ and wave functions $\{\Psi_i\}$ of quantum dots under an electric field are obtained by solving the Schrödinger equation

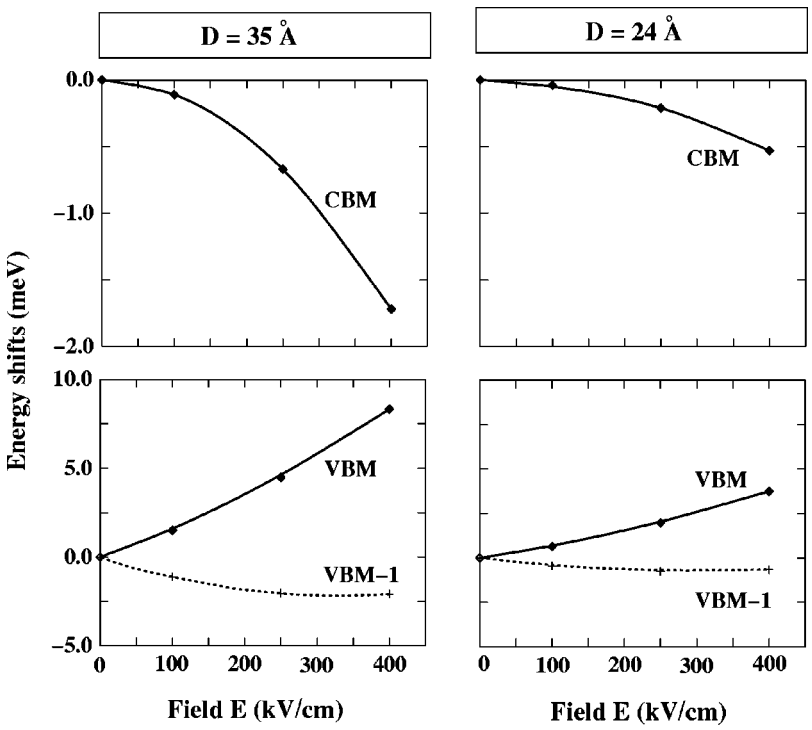

FIG. 1. Field-induced shifts of the single-particle orbital energies, for $D=35$ and 24 Å dots. Symbols are results of pseudopotential calculations; lines are guides for the eye. Note the different scales for the shifts of the CBM and VBM.

$$[-\tfrac{1}{2}\nabla^2+V_{\rm int}(\mathbf{r})+V_{\rm ext}(\mathbf{r})]\Psi_{\rm i}(\mathbf{r})=\varepsilon_{\rm i}\Psi_{\rm i}(\mathbf{r}), \qquad (2)$$

where the internal potential $V_{\rm int}(\mathbf{r})$ under zero field is a superposition of the screened atomic pseudopotentials[14] generated by all atoms in the dot, i.e., $V_{\rm int}(\mathbf{r})=\Sigma_{\rm n}v_{\rm at}(\mathbf{r}-\mathbf{R}_{\rm n})$, where $\mathbf{R}_n$ is the atomic location. The screened atomic pseudopotentials $v_{\rm at}$ were derived from first-principles density-functional calculations, and were successfully applied to semiconductor dots on a variety of physical properties such as the size dependence of the photoexcitation spectrum,[15(a)] the electron-hole exchange interaction,[15(b)] and the pressure-induced band-gap transition.[15(c)] The potential generated by the external electric field along the z direction is modeled as a sawlike potential,[13,16] i.e.,

$$V_{\rm ext}(\mathbf{r})=|e|Ez\left(-\frac{L}{2}<z\leqslant\frac{L}{2}\right), \qquad (3)$$

where E is the magnitude of the *screened* electric field, and L is the size of the supercell, chosen to be large enough so that the results will not be altered significantly. A screened electric field is used in Eq. (3), since the first-principles density-functional calculations[16] demonstrated that the charge screening of the external electric field can be well described simply by changing the slope of the external field potential. A Gaussian cutoff scheme[13] is used to smooth the discontinuity of $V_{\rm ext}(\mathbf{r})$ at the supercell boundary. The Schödinger equation in Eq. (2) is solved using the folded spectrum method.[17]

Three spherical InP dots are considered with diameters of 24, 28, and 35 Å, respectively. The electric field is applied along the cubic [001] direction of bulk InP. The atomic arrangements in the dots are assumed to be the same as in bulk InP, except that the atoms outside a certain distance from the center are truncated. The surface dangling bonds of dots are fully passivated using ligandlike atomic potentials.[14] After passivation, the band-edge states are all bulklike, with their wave functions distributed in the interiors of dots. Calculations are done with large enough supercells, for instance, a cubic supercell of $L=41$ Å is used for the 28-Å dot, and increasing the cell size from 41 to 47 Å changes the Stark shifts by less than 0.5%. The considered field strength ranges from 0 to 400 kV/cm, chosen to be comparable with the experimental values.[6]

The shifts of single-particle orbital energies of the CBM, VBM, and VBM-1 states, defined as $\Delta\varepsilon_i=\varepsilon_i(E)-\varepsilon_i(E=0)$, are shown in Fig. 1 for the 35- and 24-Å dots. Under zero field, the VBM of the spherical zinc-blende dot is doubly degenerate (with spin-orbit coupling included in the calculations). Upon the imposition of electric field, the VBM splits, as shown in Fig. 1. The band-edge valence states are expected to shift up in energy with increasing field, while the CBM is expected to shift downward, according to the single-band effective-mass theory[18] in which the signs of orbital-energy shifts are determined by effective masses. This is indeed true for the VBM and the CBM in Fig. 1. However, unlike the VBM, the VBM-1 state in Fig. 1 moves *downward* in energy, and the shift gradually saturates at high fields. The energy curvature of the VBM-1 state in Fig. 1 manifests an extensive coupling among the orbital states in strongly confined dots, caused by the perturbation of the electric field. The downward shift of the VBM-1 state is due to its interaction with the VBM state, and the saturation could come from its strong repulsion with the valence states below. Our calculations thus reveal that interstate couplings are important in affecting the quantum-confined Stark effect in colloidal dots. Although the calculations are done for spherical dots, the conclusion here should be applicable for many situations in which the energies of the two highest valence states

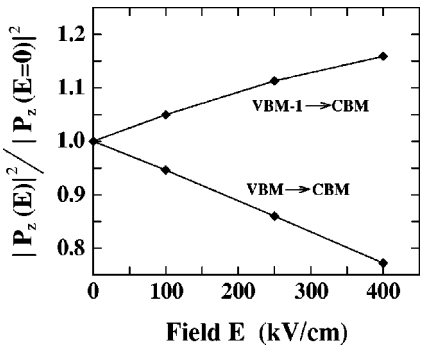

FIG. 2. Relative transition matrix elements $|P_z(E)|^2/|P_z(E=0)|^2$ for the VBM→CBM and VBM-1→CBM transitions in the $D=35$ Å dot. Symbols are the calculation results; lines are guides for the eyes.

are nearly degenerate (for example, in nearly spherical dots). We also found that, for a fixed field strength, the energy shift of the highest *p*-like valence state (the next state below the VBM-1, which is not shown in Fig. 1) is less than half of the shift of the VBM (*s*-like) in the $D=35$ Å dot. However, the shifts of the *s*- and *p*-like valence states are very close in the $D=24$ Å dot. This finding can also be explained using the interstate couplings in dots. In the $D=35$ Å dot, the energy spacing between the *p*-like valence state and the VBM-1 is small, and the repulsion between these two valence states is therefore very strong, which will substantially suppress the field-induced upward shift of the *p*-like state. Figure 1 also shows that the energy shift of the VBM in InP dot is significantly larger than that of the CBM, indicating that the VBM is much more strongly polarized. The large valence-state mixing (i.e., heavy damping) causes the strong field effect on the VBM.

The field effect on the band-edge transitions is examined by calculating the component of the transition matrix element along the field direction, i.e., $P_z(E)=\langle\Psi_{iv}|\hat{P}_z|\Psi_{jc}\rangle$. Figure 2 shows the ratio $|P_z(E)|^2/|P_z(E=0)|^2$ for the VBM→CBM and VBM-1→CBM transitions in the $D=35$ Å dot. While the VBM→CBM transition is gradually quenched by the field, the transition VBM-1→CBM is, however, intensified if a polarized excitation along the field direction is conducted. The abnormal field dependence of the VBM-1→CBM transition intensity can be understood microscopically from the wave functions of these states. The field-induced variations of the planar-averaged wave function squares,

$$\Delta\chi_i=\int\int dx\,dy[|\Psi_i(\mathbf{r};E)|^2-|\Psi_i(\mathbf{r};E=0)|^2], \quad (4)$$

are plotted in Fig. 3 for the 35-Å dot under a 250-kV/cm field. From the envelopes of the wave function variations in Fig. 3, it can be seen that the CBM and VBM are polarized along *opposite* directions, and the transition between these two states will thus be weakened by the field. However, the VBM-1 state is largely polarized *along the same direction* as the CBM, which will result in an enhancement of the optical transition. It is worth mentioning that our atomistic calcula-

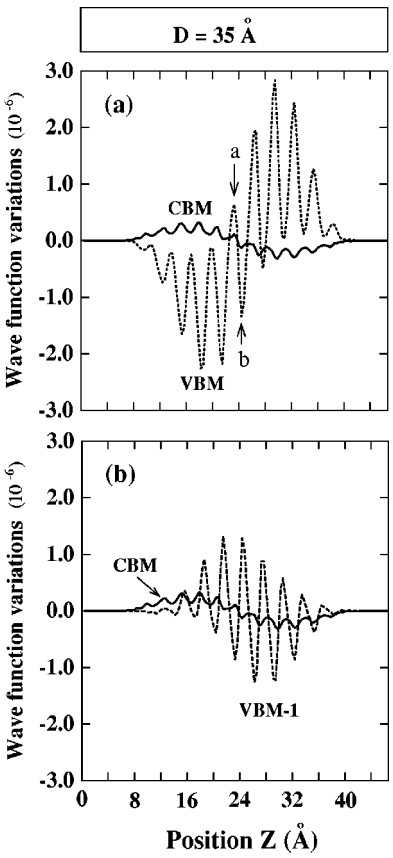

FIG. 3. Field-induced variations of planar-averaged wave-function squares for (a) the CBM and VBM states and (b) the CBM and VBM-1 states of the $D=35$ Å dot under an $E=250$ kV/cm field. The CBM state is repeated in the lower panel for comparison. The center of the dot is located at $z=23.3$ Å.

tion results in Fig. 3 also reveal a non-negligible wave-function distortion on the atomic scale in addition to the variation of the envelope part. For instance, peaks *a* and *b* in Fig. 3(a) around the central atomic layer are highly asymmetric, indicating that the atomic wave function inside a bulk primary cell is substantially polarized. The wave-function distortion on the atomic scale is neglected in the continuum electronic-structure theory.

The field-induced reductions of the single-particle energy gaps, $\Delta\omega_{\rm gap}^{\rm sp}=[\varepsilon_{\rm CBM}(E)-\varepsilon_{\rm VBM}(E)]-[\varepsilon_{\rm CBM}(E=0)-\varepsilon_{\rm VBM}(E=0)]$, and the excitonic gaps $\Delta\omega_{\rm gap}^{\rm ex}=\Delta\varepsilon_{\rm gap}^{\rm sp}-[J_{e\text{-}h}(E)-J_{e\text{-}h}(E=0)]$, where $J_{e\text{-}h}$ is the screened electron-hole Coulomb interaction, are given in Fig. 4. As a result of the distorted VBM and CBM wave functions, the Coulomb interaction $J_{e\text{-}h}$ will decrease relative to its zero-field value, and therefore, the Stark shift of the excitonic gap $\Delta\omega_{\rm gap}^{\rm ex}$ will be smaller than the field-induced reduction of the single-particle energy gap $\Delta\omega_{\rm gap}^{\rm sp}$. This is indeed born out in Fig. 4, where for the $D=24$ Å dot the Stark shifts of the excitonic gaps are found to be only half of the reductions of the single-particle gaps.

To examine the dipole and polarizability contributions to the shift of the single-particle gap ($\Delta\omega_{\rm gap}^{\rm sp}$) and to the shift of the excitonic gap ($\Delta\omega_{\rm gap}^{\rm ex}$), the relationships between

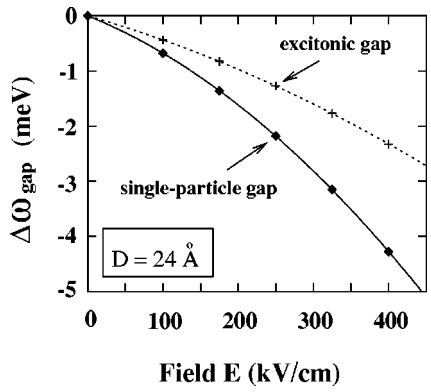

FIG. 4. Shifts of the single-particle energy gap and the excitonic gap of the $D=24$ Å dot with the field strength. Symbols are the calculation results; lines are the fitted results using Eq. (1) with the parameters given in Table I.

$\Delta\omega_{\rm gap}^{\rm sp(ex)}/E$ and the field strength E are shown in Fig. 5(a), indicating linear dependences. Extrapolating each curve in Fig. 5(a) to $E=0$ will give the value of the ''optical'' dipole μ [see Eq. (1)], while the slope of the curve will give the polarizability. Our results in Fig. 5(a) thus clearly show that even in spherical InP dots there is a dipole contribution to the Stark shift. The dipole μ and polarizability α extracted for different sizes of dots are given in Table I. It shows that both

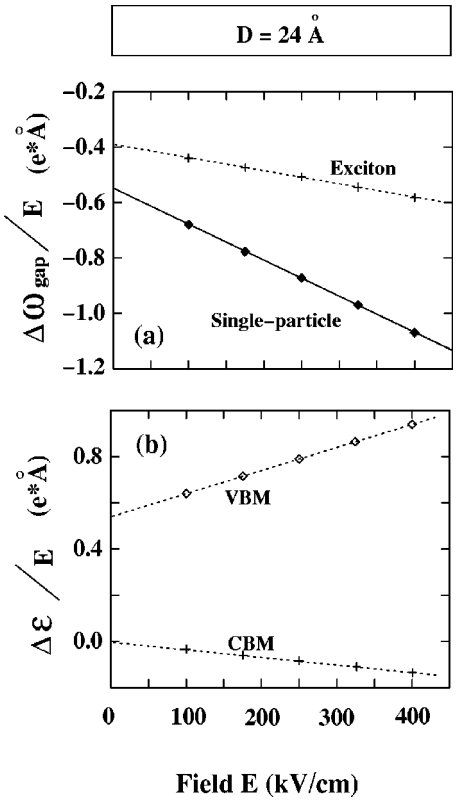

FIG. 5. Linear dependences on the field strength E of the following quantities: (a) $\Delta\omega_{\rm gap}^{\rm sp}/E$ and $\Delta\omega_{\rm gap}^{\rm ex}/E$ (the energy-gap related quantities); (b) $\Delta\varepsilon_i^{\rm sp}/E$ (where i is the CBM and VBM, the orbital-energy related quantities) for the $D=24$ Å dot. Symbols are pseudopotential calculation results; lines are linearly fitted results.

TABLE I. Dipole μ (in units of $|e|\cdot$Å) and polarizability α (in units of 10^5 Å^3) of InP dots of different sizes. The data in the second and third columns are extracted from the single-particle energy gaps, while the data in the fourth and fifth columns are extracted from the excitonic gaps.

Size (Å)	Single-particle gap		Excitonic gap	
	μ	α	μ	α
24	−0.5480	−0.4700	−0.3902	−0.1718
28	−1.2196	−0.5663	−0.6661	−0.4491
35	−1.3109	−1.0848	−0.9244	−0.6719

μ and α increase with the increasing size: semiconductor dots behave like macromolecules in their electrical properties. The calculated excitonic polarizability of the $D=35$ Å InP dot is about 0.67×10^5 Å^3, compared to the experimental value of 2.4×10^5 Å^3 in a $D=58$ Å CdSe dot.[6] The origin of the dipole contribution revealed by our calculations is somewhat puzzling from the consideration of the atomic geometry, since the spherical InP dot with T_d symmetry is not expected to exhibit any charge dipole when the electric field is applied along the cubic [001] direction. A careful analysis allows us to attribute the dipole contribution to the intrinsic degeneracy of the VBM state in a spherical zinc-blende dot under zero field. Because of the degeneracy, each orbit of the two degenerate states is *asymmetrically* distributed at two sides of the (001) plane. Stemming from the dot's orbit, the dipoles obtained here are thus ''orbital'' dipoles instead of the normal charge dipoles. This explanation about the origin of the dipolar character is further supported by Fig. 5(b), where the quantity $\Delta\varepsilon_i^{\rm sp}/E$, related to the *single-particle* orbital energy, is shown when i is the CBM state and the VBM state. Note in Fig. 5(b) that only the line for the VBM is extrapolated to a nonzero value at $E=0$, indicating that the VBM is responsible for the dipole contribution. Since the nonspherical dots will naturally introduce a geometry-related dipole, our calculations therefore suggest that all zinc-blende dots will exhibit a dipolar character in their Stark shifts.

More insight into the field effect in quantum dots can be obtained by projecting the dot states $\{\Psi_i^{\rm dot}\}$ into bulk Bloch states $\{\phi_{n\mathbf{k}}^{\rm bulk}\}$, where n is the bulk band index and $\mathbf{k}$ is wave vector of bulk Bloch state, i.e.,

$$\Psi_i^{\rm dot}(\mathbf{r})=\sum_{n\mathbf{k}} C_{n\mathbf{k}}^i \phi_{n\mathbf{k}}^{\rm bulk}, \tag{5}$$

where $C_{n\mathbf{k}}^i$ are the expansion coefficients. Equation (5) is possible since the bulk Bloch wave functions form a complete basis set. To study how an electric field affects multiband mixings, we define a band contribution $B_i(n)$, quantifying the contribution of the nth bulk band in forming the ith dot's state:

$$B_i(n)=\int d\mathbf{k}|C_{n\mathbf{k}}^i|^2. \tag{6}$$

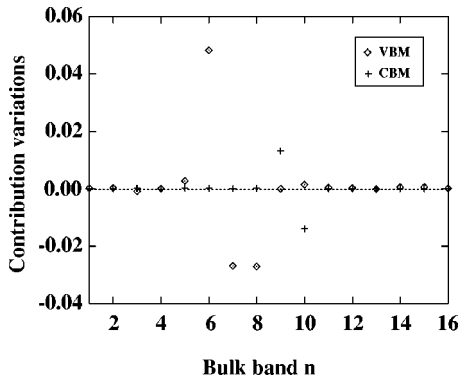

FIG. 6. Variations of bulk band contributions $\Delta B_i(n)$, induced by an $E=100$ kV/cm field, where i is the CBM (cross symbols) and the VBM (diamond symbols) of the $D=24$ Å dot.

The field-induced variations $\Delta B_i(n)=B_i(n;E)-B_i(n;E=0)$, where i is either the CBM or VBM of the $D=24$ Å dot, are shown in Fig. 6. The contributions of the lowest 16 bulk bands, i.e., $n=1-16$ (including spin-split bands), are presented. For the dot's CBM state, the contributions vary mainly between two spin-split lowest bulk conduction bands (i.e., $n=9$ and 10), indicating that the electric field triggers a change in the spin character. This is rather interesting, and it suggests that electric fields may provide a way to control the spin dynamics in dots. While the electric-field potential itself does not involve spin, it alters the spatial orbits of dots' states and causes a change in the spin character via the spin-orbit interaction. For the dot's VBM state in Fig. 6, the change in the bulk band contributions occurs among the four highest bulk valence bands. Figure 6 shows no significant contribution change across the energy gap, for both the VBM and CBM states. This is likely due to the large energy gap of the dot (~ 2.4 eV) and the small electric field applied.

In summary, we study the band-edge electronic structure of spherical InP dots under electric fields. We find that the strong interstate couplings in dots are important in affecting the field-induced changes of orbital energies and optical transitions. As a consequence of these couplings, the VBM-1 state is polarized along the same direction as the CBM, and the corresponding transition between these two states will be enhanced instead of being weakened by the electric field. We demonstrate that there are both dipole and polarizability contributions in the Stark shifts of spherical zinc-blende dots. The dipole contribution is found to be intrinsic. We also reveal that the electric field could affect the electron spin via the spin-orbit coupling.

This work was supported by the NSF, Division of Materials Research, under Grant No. DMR-0116315.

[1] L.E. Brus, J. Chem. Phys. **79**, 5566 (1983).
[2] Al.L. Efros, M. Rosen, M. Kuno, M. Nirmal, D.J. Norris, and M.G. Bawendi, Phys. Rev. B **54**, 4843 (1996).
[3] S.H. Tolbert and A.P. Alivisatos, Science **265**, 373 (1994).
[4] V.L. Colvin, K.L. Cunningham, and A.P. Alivisatos, J. Chem. Phys. **101**, 7122 (1994).
[5] A. Sacra, D.J. Norris, C.B. Murray, and M.G. Bawendi, J. Chem. Phys. **103**, 5236 (1995).
[6] S.A. Empedocles and M.G. Bawendi, Science **278**, 2114 (1997).
[7] C.A. Leatherdale, C.R. Kagan, N.Y. Morgan, S.A. Empedocles, M.A. Kastner, and M.G. Bawendi, Phys. Rev. B **62**, 2669 (2000).
[8] D.A.B. Miller, D.S. Chemla, and S. Schmitt-Rink, Appl. Phys. Lett. **52**, 2154 (1988).
[9] T.D. Krauss and L.E. Brus, Phys. Rev. Lett. **83**, 4840 (1999).
[10] M. Nirmal, B.O. Dabbousi, M.G. Bawendi, J.J. Macklin, J.K. Trautman, T.D. Harris, and L.E. Brus, Nature (London) **383**, 802 (1996).
[11] Al.L. Efros and M. Rosen, Phys. Rev. Lett. **78**, 1110 (1997).
[12] L.-W. Wang, J. Phys. Chem. B **105**, 2360 (2001).
[13] H. Fu, Phys. Rev. B **64**, 075303 (2001).
[14] H. Fu and A. Zunger, Phys. Rev. B **55**, 1642 (1997).
[15] (a) L.-W. Wang and A. Zunger, J. Phys. Chem. B **102**, 6449 (1998); (b) A. Franceschetti, L.-W. Wang, H. Fu, and A. Zunger, Phys. Rev. B **58**, R13 367 (1998); (c) H. Fu and A. Zunger, Phys. Rev. Lett. **80**, 5397 (1998).
[16] K. Kunc and R. Resta, Phys. Rev. Lett. **48**, 406 (1982).
[17] L.-W. Wang and A. Zunger, J. Chem. Phys. **100**, 2394 (1994).
[18] G. Bastard, E.E. Mendez, L.L. Chang, and L. Esaki, Phys. Rev. B **28**, 3241 (1983).